An Experimental Study on the Measurement of Fuel to Air Ratio Using Flame Chemiluminescence

Sewon Kim, Chang Yeop Lee, Minjun Kwon

Abstract—This study is aiming at establishing the relationship between the optical signal of flame and an equivalent ratio of flame. In this experiment, flame optical signal in a furnace is measured using photodiode. The combustion system is composed of metal fiber burner and vertical furnace, and flame chemiluminescence is measured at various experimental conditions. In this study, the flame chemiluminescence of laminar premixed flame is measured using commercially available photodiode. It is experimentally investigated the relationship between equivalent ratio and photodiode signal. In addition, the strategy of combustion control method is proposed using the optical signal and fuel pressure.

The results showed that certain relationship between optical data of photodiode and equivalence ratio exists, and this leads to the successful application of this system for instantaneous measurement of equivalence ration of the combustion system.

Keywords—Flame chemiluminescence, photo diode, equivalence ratio, combustion control.

I. INTRODUCTION

THE present study is aiming at establishing high efficiency and low pollutant combustion system by measuring and controlling air to fuel ratio in real time [1]. Thus, there are growing interests for precise and real time combustion control technologies. In particular, many researchers have been conducted on the development of real time equivalence ratio sensor in order to increase the efficiency of combustion system such as industrial furnace, industrial boiler and domestic boiler.

A responsive sensor is required for real time combustion control of combustion systems. However, the existing sensors, such as zirconia type oxygen sensor, cannot be applied to real time combustion control because they have flue gas flow time delay and time delay of sensor itself.

Optical measurement techniques of flame chemiluminescence are useful to apply to combustion control because of their short response time.

Higgins [2], [3] et al. derived the relationship between two radicals, OH*, CH*, and equivalent ratio. Thus they expressed the relationship as a function of temperature and pressure.

Kojima [4], and Ikeda [5] et al. found the linear relationship between equivalent ratio and flame chemiluminescence ratio on laminar premixed flame, and they derived that this relationship can be applied to turbulent premixed flame and diffusion flame.

Muruganandam [6], [7] et al. derived the linear relationship between equivalent ratio and radical of specific chemical

Sewon Kim and Changyeop Lee are with Korea Institute of Industrial Technology, Cheonan, Chungnam, Korea (e-mail: swkim@kitech.re.kr, cylee@kitech.re.kr).

Minjun Kwon is with the Hanyang University, Seoul, Korea (phone: +82-41-589-8533; fax: +82-41-589-8548; e-mail: mjk@kitech.re.kr).

species, and they suggested the possibility of application to the combustion control of gas turbine combustor.

The optical measurements are conducted at premixed flames formed using metal fiber burner. The flame optical measurement is performed using commercially available photo diode element.

An extensive experimental works are conducted to derive the relationship between optic signal of photo diode and flame operating condition, such as fuel to air ratio.

II. FUNDAMENTAL THEORIES

A. Flame Chemiluminescence

Fig. 1 is flame spectral analysis at UV and VIS region (wavelength: 200nm~550nm). There are three large peaks OH, CH, C_2, respectively. The center wavelength of each peak are 308nm (OH), 431nm (CH), 515nm (C_2) approximately [8]. In a recent study, the mainly targets of the radicals are OH, CH, C_2. In particular, the radicals of CH and C_2 have a relatively large peak and the CO_2 radical and blackbody radiation of soot are present in all wavelengths.

Fig. 2 shows the relative emission definition of the CH radical. As shown in the figure, CO_2 radical appear in all wavelength range. And the blackbody radiation influence of soot radical is displayed depend on the temperature and the wavelength.

At various temperatures for the blackbody radiation according to wavelength is shown in Fig. 3. As shown in the figure 400nm wavelength of the blackbody radiation energy is the effect of temperature is very small.
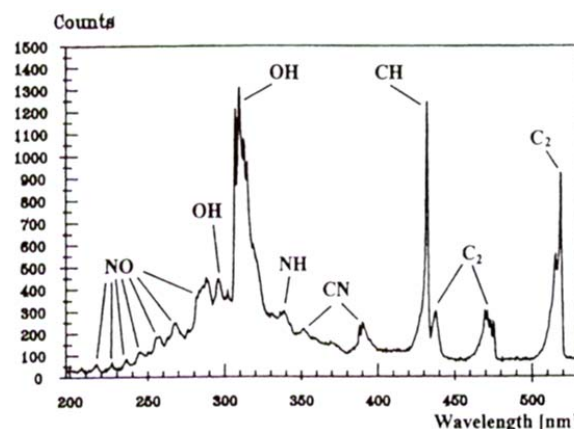

Fig. 1 Flame spectral analysis at UV and VIS region

The blackbody radiation, however, is suddenly increased in the wavelength region over 500nm. Therefore when measuring

World Academy of Science, Engineering and Technology
International Journal of Chemical and Molecular Engineering
Vol:8, No:2, 2014

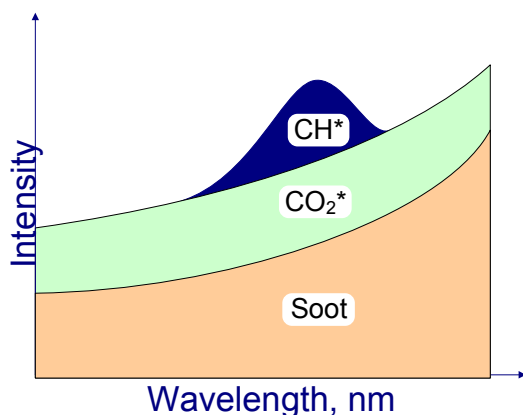the flame chemiluminescence the blackbody radiation affect as a noise at long wavelength region (over 500nm).
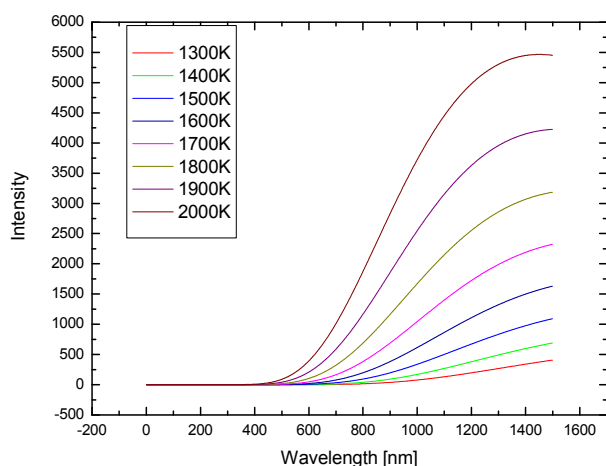
Fig. 2 CH* relative emission definition

Fig. 3 Plank's curve for various temperatures

III. EXPERIMENTAL SETUP

A. Experimental System

Fig. 4 is the schematic diagram of experimental system. The experimental system comprise metal fiber burner, experimental furnace, fuel supply system, optical sensor, stack gas analyzer and control system.

The metal fiber burner (Fig. 7) commonly is applied to household boiler. The burner forms the laminar premixed flame. So the flame is very small. In this study, the burner is commercial model. Max. Load is 39,000kcal/h and applied fuel is LNG.

The experimental furnace is circular vertical furnace and inside was coated with refractory material. The inner diameter of the Experimental furnace is 450mm and has a length of 1400mm. The optical measurement is performed through the observation window on the side (Fig. 9).

There are fuel flow meter and pressure sensor in fuel supply system. P1 is pressure of supplying LNG before flow meter and P2 is the pressure after flowmeter. In this study, MFM is applied as a fuel flowmeter; pressure transducer is applied as

pressure sensor. These sensors signal are acquired and saved by control system on real time.

The Stack gas analyzer is type of chemical cell. It measures CO, NO_X, and O_2. And the concentration data of each species is acquired and saved by control system.

The control system perform data acquisition and burner control. The acquired data are fuel flow rate, pressure at before MFM (P1), pressure at after MFM (P2), fuel temperature, PD signal, PD operating temperature, furnace temperature, and concentration of species in stack. These data are acquired and saved on real time.

There are specific data of PD in Table I. The wavelength of peak sensitivity is 280nm - UV range enhanced, range of spectral bandwidth is 210~380nm, the angle of half sensitivity is ±10.

Fig. 4 shows the spectral response of PD (black line) and flame chemiluminescence (blue line). There are three the large peaks as OH, CH and C_2 on blue line. As shown in the figure, the spectral response of PD includes only OH radical. This region called UV region is less affected by blackbody radiation. Fig. 6 shows the field of view on PD.

TABLE I
THE SPECIFIC DATA OF PHOTO DIODE

Variables	Range of values
Wavelength of peak sensitivity λ peak (nm)	280
Range of spectral bandwidth λ 0.5 (nm)	210~380
Angle of half sensitivity(degree)	±10

B. Experimental Condition

The experimental variables are load, flue gas O_2, PD sensor height. The values of variable are shown in Table II. In particular, the equivalent ratio can be expressed in flue gas O_2. When the state of combustion investigates, the most useful information is a concentration of flue gas O_2.In fact, excess air and equivalent ratio can be derived from the concentration of flue gas O_2. Therefore in this study, instead of the equivalence ratio of the combustion conditions to apply to concentration of flue gas O_2.

A type of fuel in this research is commercial LNG. The load variations are 25000, 30000, 35000, 39000 kcal/h. The range of flue gas O_2 is 1 to 5 percent. Fig. 9 is a diagram of sensor height. Because PD has a detection angle, there is optimal location for detecting.

In this research prove the response of PD and finding the optimal detecting location. Then the response is evaluated about external factors such as furnace temperature, PD operating temperature.

Finally, build a database on the burner on each condition, and derive the relationship between PD signal and burner condition.

IV. RESULTS

A. Burner Operating

From Figs. 10-12 are picture of flame on metal fiber burner. Fig. 10 shows the flame different load respectively. The main flame is on the burner but there is the stream of flame. As it can be deduced from Fig. 10, the length of the stream increases with

World Academy of Science, Engineering and Technology
International Journal of Chemical and Molecular Engineering
Vol:8, No:2, 2014

the increase of load.

Figs. 11 and 12 show the flame on metal fiber burner different concentration of flue gas O_2 at 30,000kcal/h and at 39,000kcal/h respectively. As shown in these figures, the blue flame increases and the length of the stream decreases when the concentration of flue gas O_2 increases.
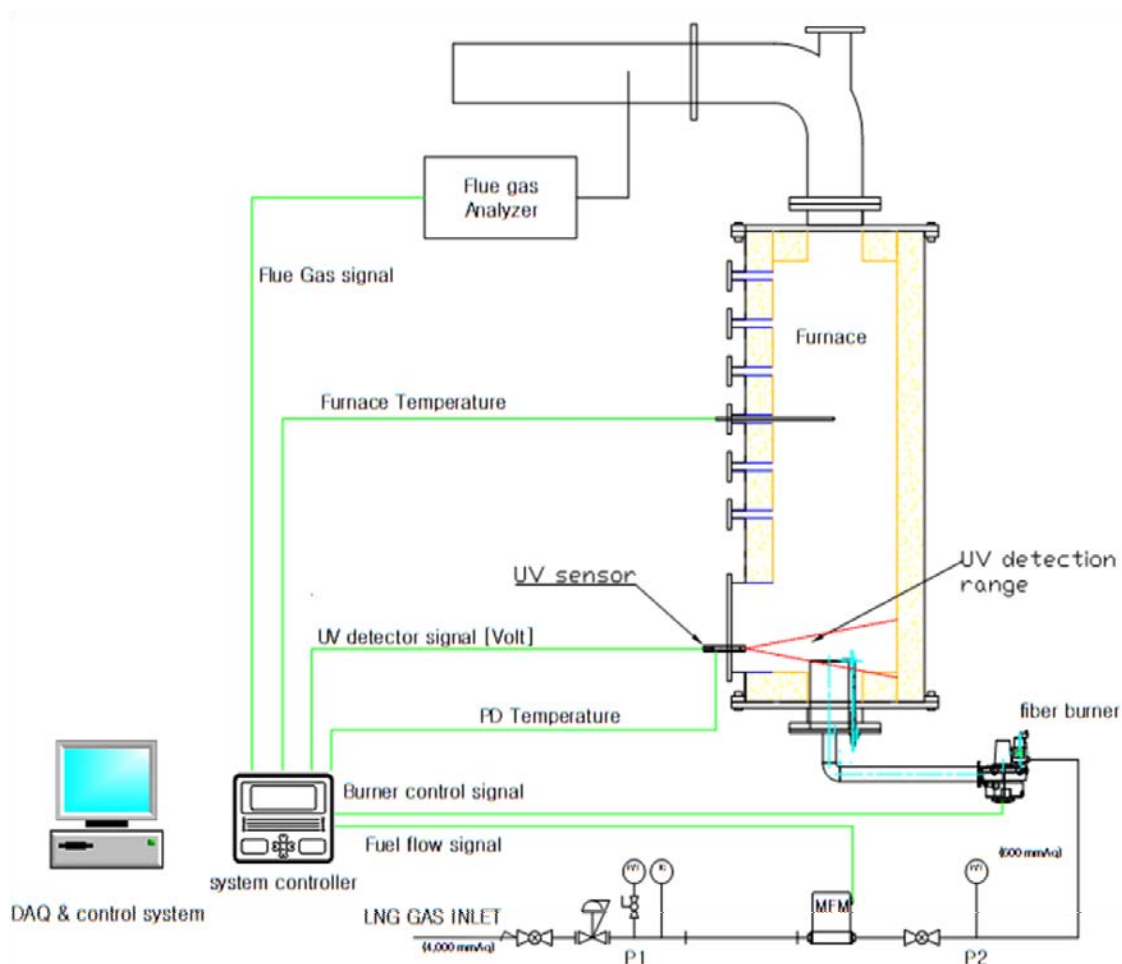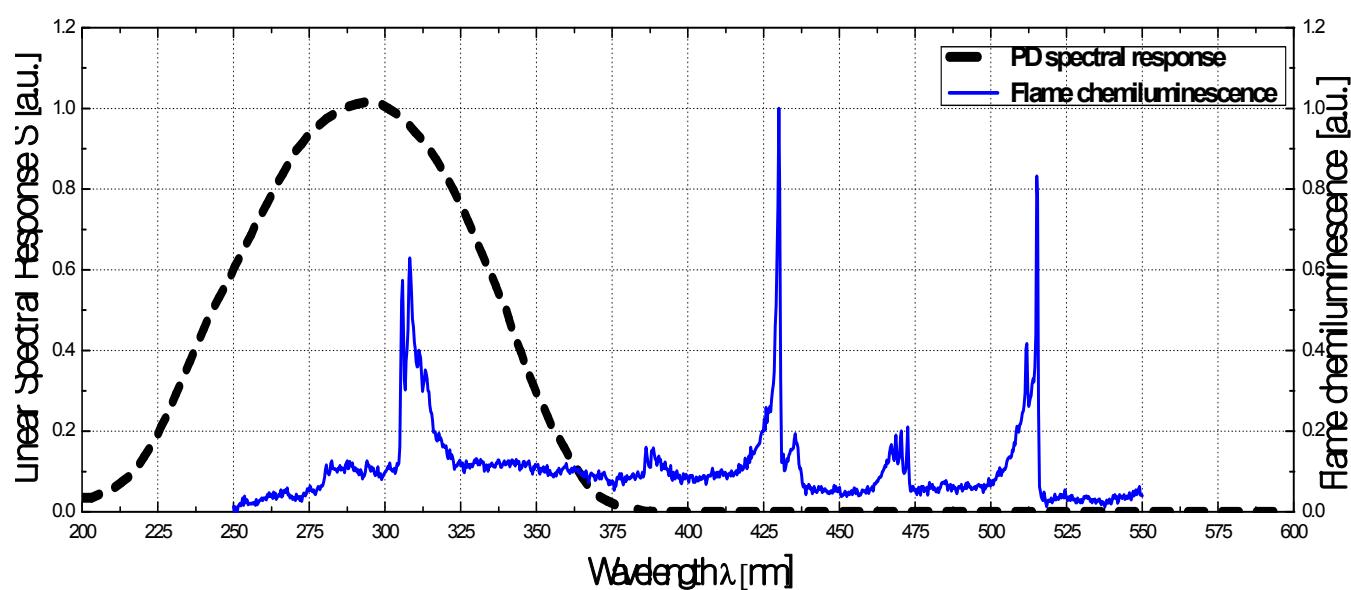
Fig. 4 Schematic diagram of experimental system

Fig. 5 Spectral Response of PD and flame chemiluminescence

World Academy of Science, Engineering and Technology
International Journal of Chemical and Molecular Engineering
Vol:8, No:2, 2014
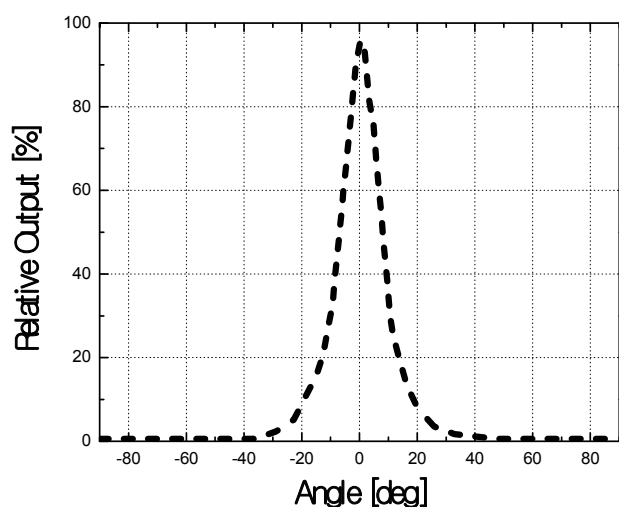
Fig. 6 Field of view on PD

TABLE II
EXPERIMENTAL CONDITIONS

Variables	Range of values
Fuel	Commercial LNG
Load [kcal/h]	25000, 30000, 35000, 39000
Flue gas O_2 [%]	1~5 %
PD sensor height [mm]	0~50mm
PD data rate[samples/sec]	2
Stack gas analyzer data rate[samples/sec]	1

Fig. 8 Picture of vertical furnace

Fig. 7 Picture of metal fiber burner
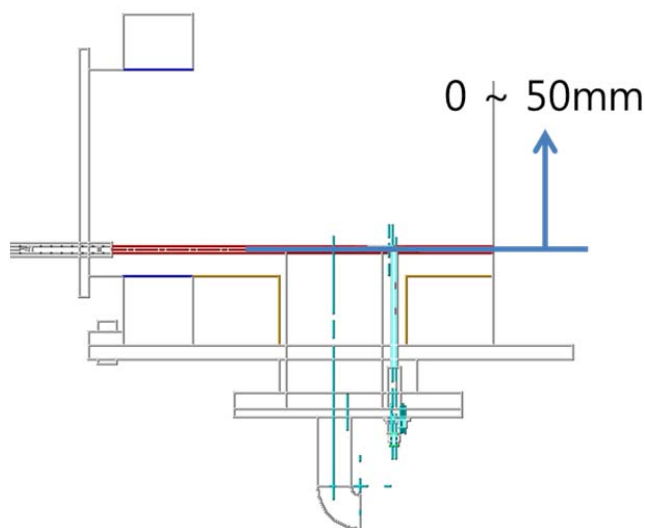
Fig. 9 Variation of sensor height

B. Optimize Detecting Location

The sensitivity angle of the PD is narrow. So there are different signal in same condition according to measuring height. Thus the optimization for measurement location is required. Fig. 13 is a graph of the PD signal for measurement location. As shown in figure the highest signal is at 10mm. This phenomenon is an effect of the metal fiber burner flame length and flame characteristics that the OH radical appear most frequently on the surface of the flame.
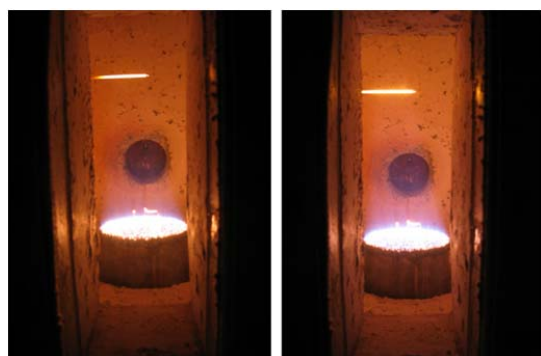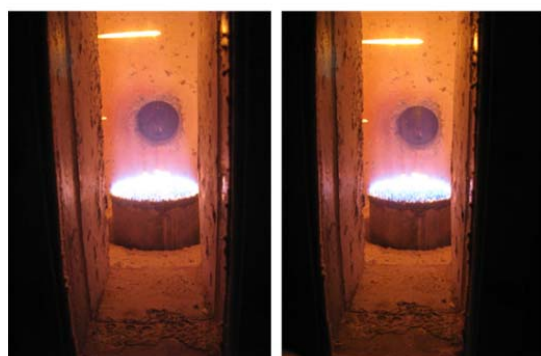
C. Sensor Response Rate

In order to measure the response time of the PD signal, stack gas analyzer, PD measurement and measuring fuel flow rate were performed at the same time. Fig. 9 is the graph at burner ignition; Fig. 10 is the graph at burner extinction. The data rate is 2 Samples/sec. The delay time is a term from time of combustion condition change to time of signal change. As the results, during ignition, the delay time of PD is 1second and the delay time of gas analyzer is 5second. During extinguishment, the delay time of PD is 0 second and the delay time of gas analyzer is 8 seconds.
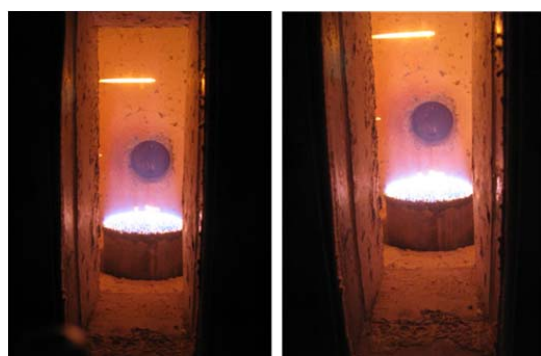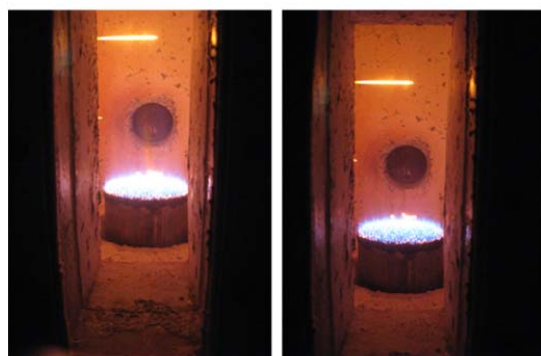
World Academy of Science, Engineering and Technology
International Journal of Chemical and Molecular Engineering
Vol:8, No:2, 2014

Fig. 10 Pictures of flame each load (@ flue gas O_2 3%)

Fig. 11 Pictures of flame each flue gas O_2% (@ 30,000kcal/h)
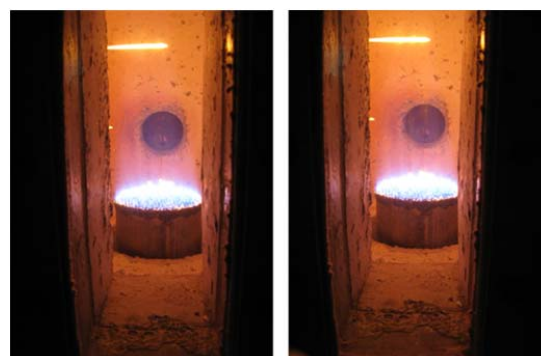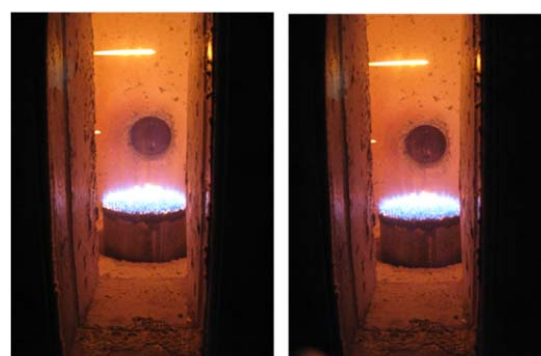
Fig. 12 Pictures of flame each flue gas O_2% (@ 39,000kcal/h)
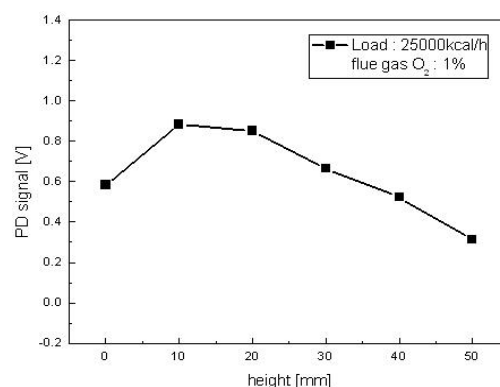
Fig. 13 PD signal for sensor height

Fig. 14 Sensor response rate on ignition

World Academy of Science, Engineering and Technology
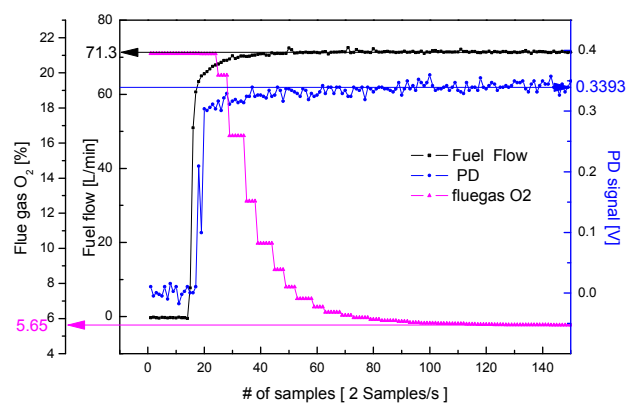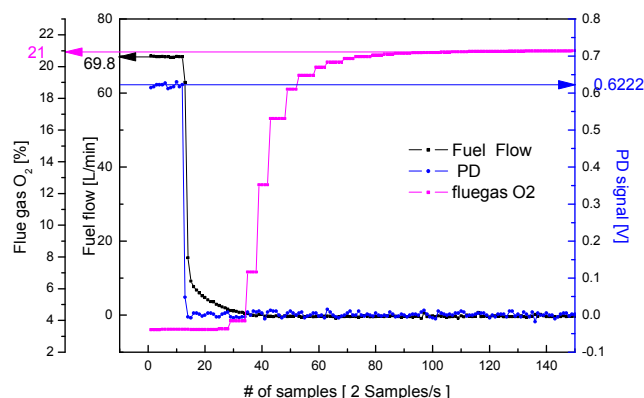International Journal of Chemical and Molecular Engineering
Vol:8, No:2, 2014

Fig. 15 Sensor response rate on extinguishment

D. Effect of Temperature

Due to the characteristic of the optical element is sensitive to temperature. Thus there is the potential to change the PD signal depending on the temperature. Also as mentioned above, blackbody radiation depend on the temperature in all of wavelength range. In this case, the furnace wall emits the blackbody radiation. So, on the effects of radiation of furnace wall check is required.

Fig. 16 shows the PD signal according to the furnace temperature. Furnace temperature measured at core of the furnace displayed on Fig. 4. According to the result, the PD signal is not depend on the furnace temperature because the PD enhanced UV range and the effect of blackbody radiation effect is very small in UV range.

Fig. 17 shows the effect of PD temperature for PD signal. The PD temperature is measured at the side of the PD element. The result show that PD signal does not depend on the PD temperature under 60°C. So when measured PD signal is required cooling of PD element.

E. PD Signal for Flue Gas O_2 at Each Load

To characterize the optical signal of the fiber burner used in this study database has built PD signal results in each load for each flue gas O_2 (Fig. 18).

The PD signal is decrease linearly when flue gas O_2 is increase in each load. And the PD signal is increase when the load is increase. According to these results, the PD signal as a tracer of the flue gas O_2 is applicable.
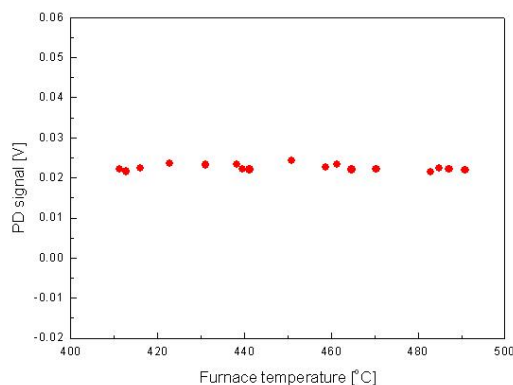

Fig. 16 Effect of furnace temperature for PD signal

F. Derive the Relationship between PD Signal and Flue Gas O_2

Fig. 19 shows the result of the linear fit to the result of Fig. 18. According the results, these lines have different slopes and intercept at each load respectively. The result of linear fit is shown Table II. The lines have different slopes and different intercept at different load conditions, but these lines can be expressed in small error.

The results of Fig. 19 are straight lines. So, we can express (1) where 'A' is the slope, 'Y' is the intercept. 'A' and 'Y' are function of load.
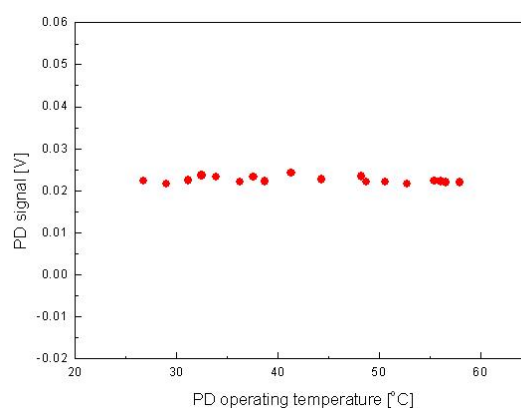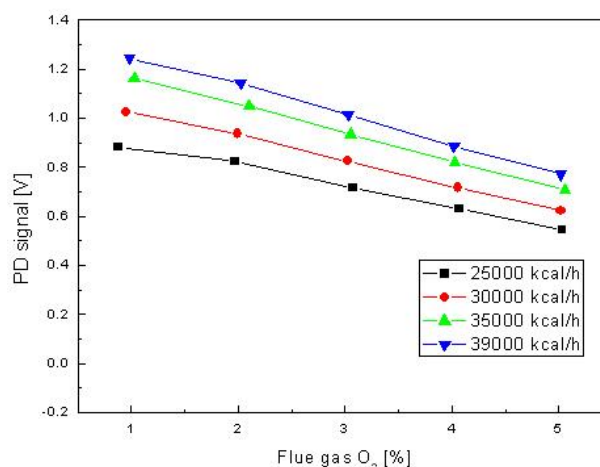

Fig. 17 Effect of PD temperature for PD signal

Fig. 18 PD signal for flue gas O_2 at each load

As it has been described in Section IV so far, 'A (slope)' and 'Y (intercept)' are different depending on the load. In this study, 'A' and 'Y' expressed as a function of load. Therefore Fig. 20 shows the polynomial fitted (2nd order) slope for load. Equation (2) is expressed 'A' function of load. Fig. 21 is the result of the polynomial fitted (3rd order) intercept for load. And equation shown in Fig. 21 shows the 'Y' function of load. The result of Fig. 20 seems as expected whereas the result of Fig. 21 is not as anticipated. Because, the number of data of 'Y' is not enough to 3rd order fit. However, the result of Fig. 21 is agreed to accept because the focus of this study is method of deriving relationship.

World Academy of Science, Engineering and Technology
International Journal of Chemical and Molecular Engineering
Vol:8, No:2, 2014

'A' and 'Y' are function of load. Most of the actual combustion system does not have a fuel flow meter. Thus, a new parameter for prediction of load is required. In this study, the fuel pressure is introduced to the parameters for the prediction of fuel flow. As described at experimental system, the parameters of fuel pressure have P1 and P2. Figs. 17 and 18 show the results of linear fit. The relationship between P1, P2 and load is shown by equations given in Figs. 22 and 23.

Fig. 24 shows the result of measuring flue gas O_2 using stack gas analyzer and the result of predicting flue gas O_2 using derived equations. The error of result applying P1 is about 0.1, and the error of result applying P2 is about 0.06. In real system, this error is relatively small errors. In terms of time, the result using stack gas analyzer is the delay time for about 5 seconds, the signal is stable, which takes about 20 seconds, but the delay is not the result using PD, stable signal, which takes about 4 seconds.
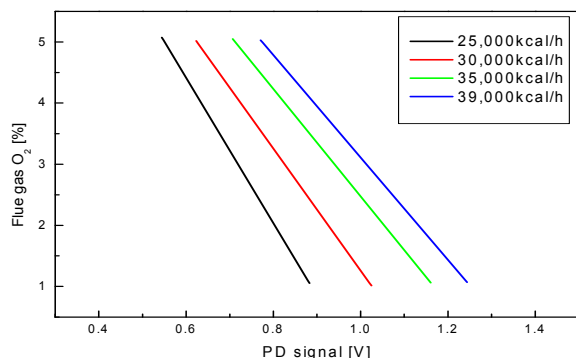
TABLE III
LINEAR FIT RESULTS

Load [kcal/h]	Slope	Intercept	R^2
25,000	-11.89	11.55	0.9907
30,000	-9.96	11.22	0.9984
35,000	-8.79	11.26	0.9992
39,000	-8.37	11.48	0.9970

$$Flue\ gas\ O_2 = A \times (PD\ Signal[V]) + Y \tag{1}$$

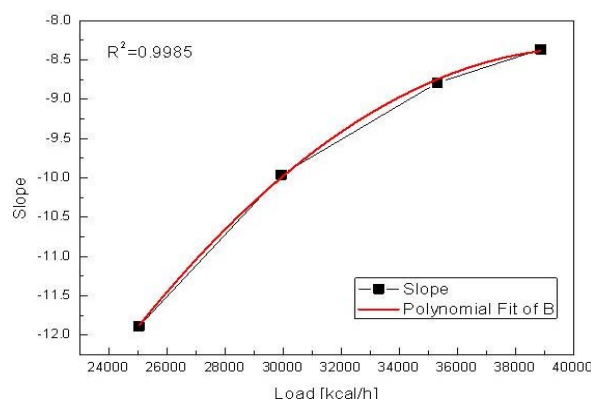where, A= Slope (function of load) B= Intercept (function of load).

Fig. 20 Polynomial fitted slope for load
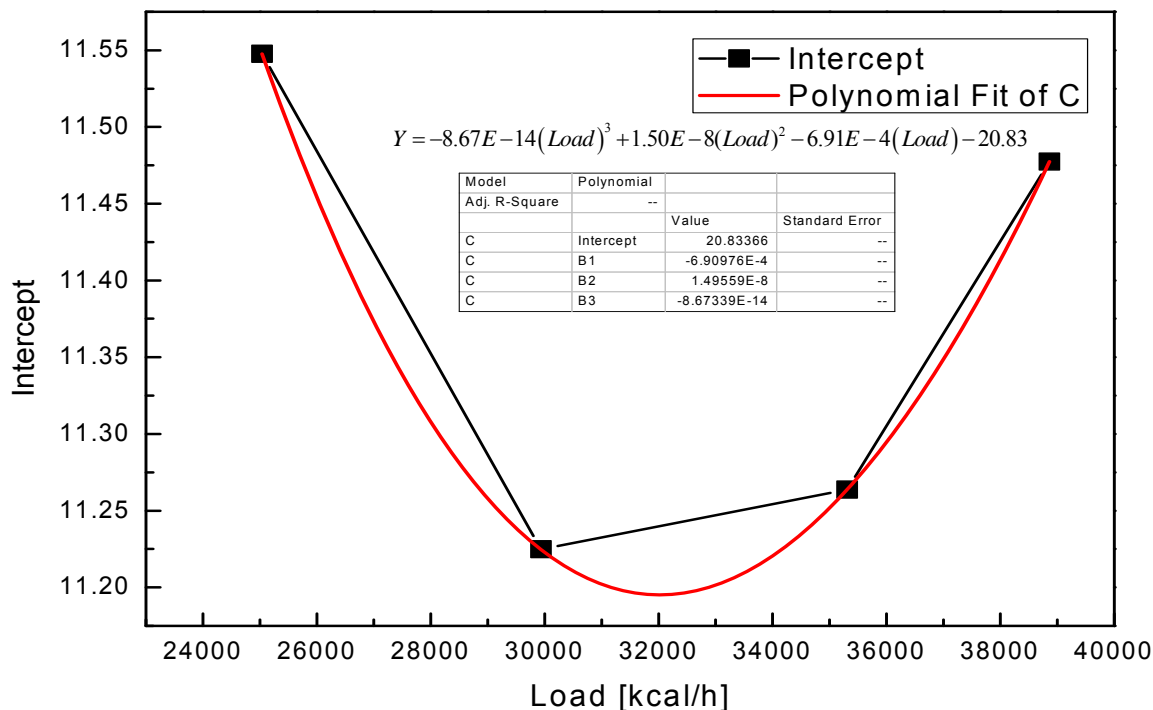
$$A = -1.47E-8(Load)^2 + 1.19E-3(Load) - 32.51 \tag{2}$$

Fig. 19 Linear fitted flue gas O_2 for PD signal at each load

$$Y = -8.67E-14(Load)^3 + 1.50E-8(Load)^2 - 6.91E-4(Load) - 20.83$$

Model	Polynomial		
Adj. R-Square		--	
		Value	Standard Error
C	Intercept	20.83366	--
C	B1	-6.90976E-4	--
C	B2	1.49559E-8	--
C	B3	-8.67339E-14	--

Fig. 21 Polynomial fitted intercept for load

World Academy of Science, Engineering and Technology
International Journal of Chemical and Molecular Engineering
Vol:8, No:2, 2014
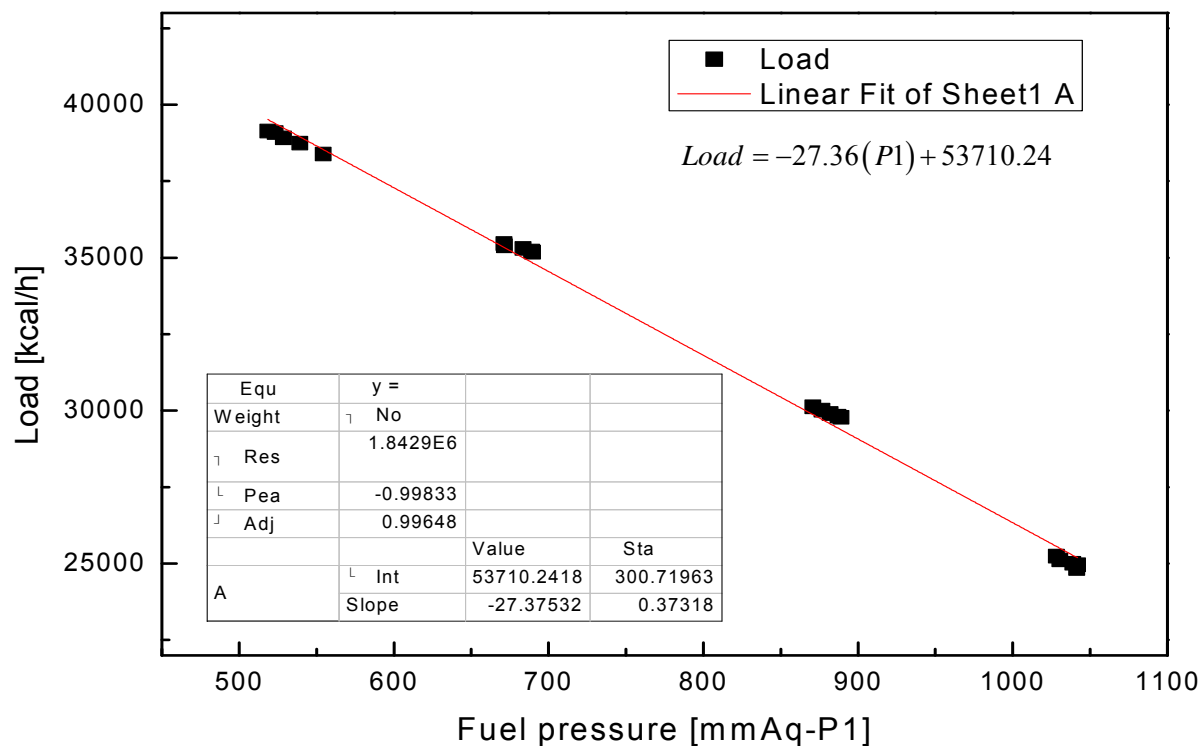
Fig. 22 Linear fitted load for fuel pressure (P1)
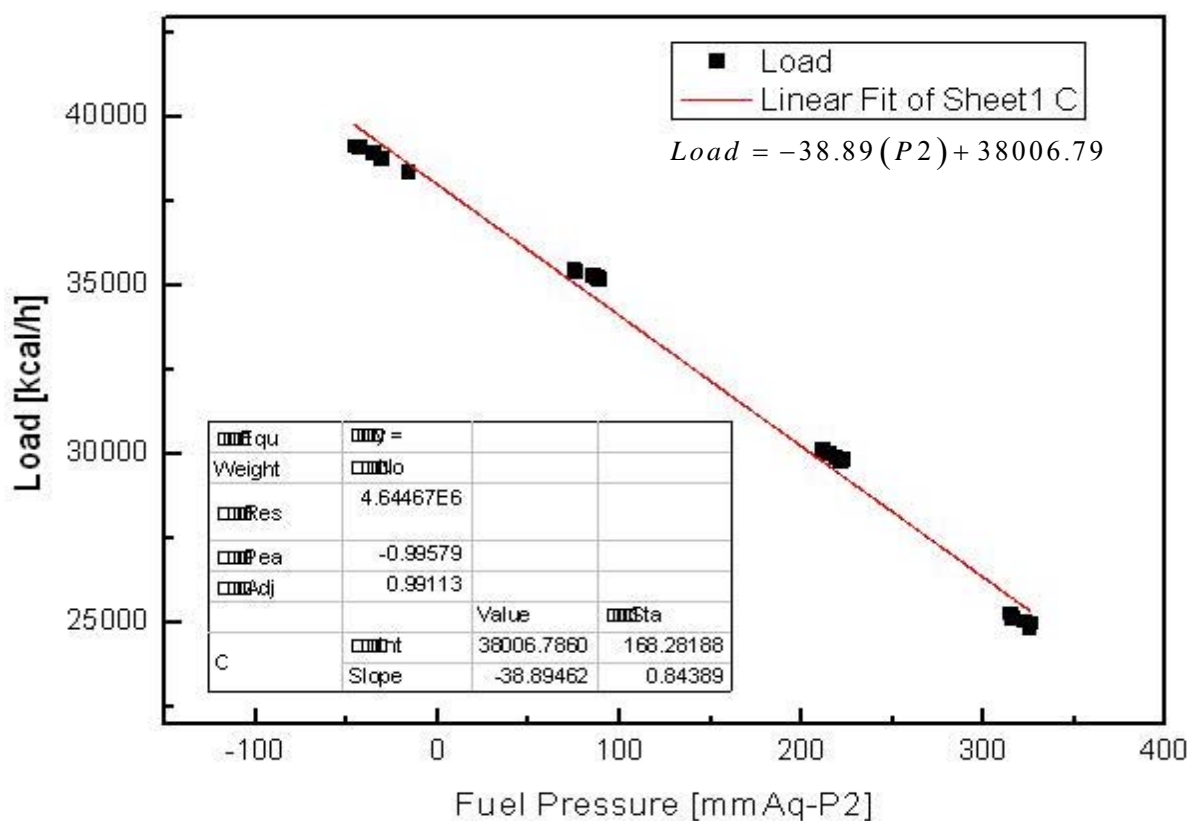
Fig. 23 Linear fitted load for fuel pressure (P2)

World Academy of Science, Engineering and Technology
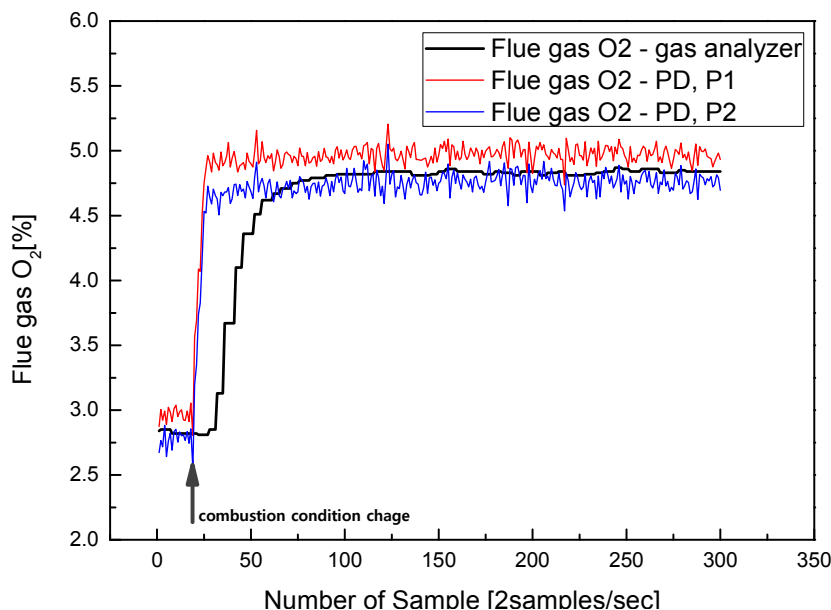International Journal of Chemical and Molecular Engineering
Vol:8, No:2, 2014

Fig. 24 Real time measurement of PD & gas analyzer

V. CONCLUSION

This study is on the measurement of the flame chemiluminescence and deriving the relationship between optical signal of flame and the state of the flame. The premixed flame using metal fiber burner is measured using the UV enhanced photo diode element. It is experimentally investigated that certain relationship between equivalent ratio and photodiode signal exists. In addition, the strategy of combustion control method is proposed using the optical signal and fuel pressure.

Finally, the optic signal of the flame and burner operating parameters are experimentally investigated, and the results are as follows.

1. During ignition, the delay time of PD is 1second and the delay time of gas analyzer is 5second. During extinguishment, the delay time of PD is 0second and the delay time of gas analyzer is 8second. (Figs. 14 and 15)
2. The PD signal is not depend on the furnace temperature because the PD enhanced UV range and the effect of blackbody radiation effect is very small in UV range (Fig. 16).
3. The PD signal is not depend on the PD temperature under 60°C (Fig. 17).
4. The PD signal of the metal fiber burner is expressed linearly at each load for flue gas O_2 (Fig. 18).
5. The PD signal as a tracer of the flue gas O_2 is applicable.
6. Derived the equation of the relationship between PD signal and flue gas O_2 using fuel pressure.
7. The result of measuring flue gas O2 using PD signal and derived equations has low error and fast response (Fig. 24).

ACKNOWLEDGMENT

REFERENCES

[1] Sewon Kim, Chang Yeop Lee, Minjun Kwon, "Real-time Integrated control system to improve boiler efficiency," Research of Energy Efficiency & Resources, Annual report in 2013.
[2] B. Higgins., M. Q. McQuay., F. Lacas., J. C. Rolon., N. Darabiga., S. Candel., "Systematic Measurements of OH Chemiluminescence for Fuel-lean, High-pressure, Premixed, Laminar Flames," Fuel Vol.80, 2001, pp. 67~74 .
[3] B. Higgins., M. Q. McQuay., F. Lacas., S. Candel., "An Experimental Study on the Effect of Pressure and Strain Rate on CH Chemiluminescence of Premixed Fuel-lean Methane/air Flames," Fuel Vol.80, 2001, pp. 1583~1591.
[4] J. Kohima., Y Ikeda., T. Nakajima., "Spatially Resolved Measurement of OH*, CH*, and C2* Chemiluminescence in the Reaction Zone of Laminar Methane/air Premixed Flames," Proc. of the Combustion Institute, Vol.28, 2000, pp.1757~1764.
[5] Y. Ikeda., J. Kojima., T Nakajima, F Akamatsu, M. Katsuki, "Measurement of the Local Flamefront Structure of Turbulent Premixed Flames by Local Chemiluminescence," Proc. of the Combustion Institute, Vol.28, 2000, pp. 343~350.
[6] T. M. Muruganandam., B. Kim., R. Olsen., M. Patel., B. Roming., J. M. Seizman, "Chemiluminescence Based Sensor for Turbine Engines", Proc. 39th Aerospace Sciences Meeting & Exhibit, 2003.
[7] Y. Hardalupas., M. Orain., C. S. Panoutsos, A.M.K.P. Taylor, J. Olofsson, H. Seyfried, M. Richter, J. Hult, M. Alden, F. Hermann, J. Klingmann, "Chemiluminescence sensor for local equivalence ratio of reacting mixtures of fuel and air(FLAMESEEK)," Applied Thermal Engineering, Vol.24, 2004, pp. 1619~1632.
[8] C. Romero., X. Li., S. Keyvan., R. Rossow., "Spectrometer-based Combustion Monitoring for Flame Stoichiometry and Temperature Control," Applied Thermal Engineering Vol. 25, 2004 pp. 659~676 .